Evidence for protein 4.1B acting as a metastasis suppressor

Tamara Cavanna[1], Eva Pokorná[2], Pavel Veselý[2], Colin Gray[1] and Daniel Zicha[1,*]

[1]Light Microscopy, Cancer Research UK London Research Institute, Lincoln's Inn Fields Laboratories, 44 Lincoln's Inn Fields, London, WC2A 3PX, UK
[2]Institute of Molecular Genetics, Academy of Sciences of the Czech Republic, Flemingovo nám. 2, 166 37 Prague 6, Czech Republic
*Author for correspondence (e-mail: daniel.zicha@cancer.org.uk)

Accepted 30 November 2006
Journal of Cell Science 120, 606-616 Published by The Company of Biologists 2007
doi:10.1242/jcs.000273

Summary

We compared a non-metastasising sarcoma cell population with three related populations of increasing metastatic potential. The metastatic cells in vitro exhibited a significantly reduced incidence of actin stress fibres but enhanced motility and chemotaxis. We also investigated gene expression underlying progression to a metastatic phenotype by performing a microarray analysis of the four sarcoma populations. We identified a subset of genes with significantly altered expression levels between non-metastasising and metastasising cells in tissue culture and in primary tumours. One such gene, encoding protein 4.1B, is downregulated in the metastatic sarcoma populations. To investigate possible roles of 4.1B in the mechanisms of metastasis, we used RNA interference (RNAi) to reduce its expression in the non-metastatic cells. Cells with reduced 4.1B expression displayed an altered F-actin morphology, with significantly fewer stress fibres. We also found that the 4.1B RNAi cells migrated at twice the speed of the untreated cells. Metastatic cells exogenously expressing 4.1B migrated at half the speed of control metastatic cells and displayed suppressed chemotaxis. Therefore, we propose that the reduction of 4.1B in the metastatic cells promotes the metastatic phenotype as a result of inducing a loss of actin stress fibres and a concomitant increase in cell motility.

Supplementary material available online at
http://jcs.biologists.org/cgi/content/full/120/4/606/DC1

Key words: 4.1B protein, Metastasis, Stress fibres, Microarray, Migration

Introduction

Metastasis, the spread of cancer from its place of origin to a secondary site, is the major cause of death in cancer patients. Therefore, identification of the genes underlying the mechanisms of metastasis is of great interest. To metastasise, tumour cells need to progress through a series of critical steps known as the metastatic cascade (Ahmad and Hart, 1997). The metastatic cascade involves the detachment of cells from the primary tumour into the surrounding tissue, intravasation into the blood or lymphatic system where they are transported, arrest in a capillary bed, extravasation and, finally, the survival and division of the tumour cells at the secondary site. Just as the interplay of tumour suppressor and promoter genes makes a cell become cancerous, so the development of metastasis requires a combination of genes whose altered expression levels allow its progress through the metastatic cascade. The development of microarray technology has enabled investigation of the changes in gene expression required for a tumour cell to metastasise. van't Veer et al. undertook a microarray analysis of breast tumours from 117 patients and identified a gene expression signature of poor prognosis (van't Veer et al., 2002). When this signature was used to predict the clinical outcome of another cohort of breast cancer patients, it outperformed all other methods of predicting the likelihood of distant metastases within five years (van de Vijver et al., 2002). A similar study with 279 diverse primary human tumours also resulted in a more accurate prognosis associated with metastasis (Ramaswamy et al., 2003). Such microarray analyses are useful to predict clinical outcomes, but there are drawbacks. For example, microarray data from patients is of limited value for identifying the expression changes mediating the progression from a benign to a metastatic tumour, because in most cases, only one sample per patient is available. Furthermore, Ein-Dor et al. recently reported that thousands, rather than hundreds, of samples are required to produce robust gene expression signatures from patients (Ein-Dor et al., 2006).

Animal models can circumvent some of the issues which complicate patient-based experiments, and have been used to implicate RhoA (Clark et al., 2000), RhoGDI2 (Gildea et al., 2002), and Ezrin (Khanna et al., 2004) as metastasis-associated proteins. Here, we used a rat sarcoma model derived by tumour progression from spontaneously transformed cells (Vesely et al., 1987). This model has specific advantages for microarray analysis of metastasis. First, it is composed of a panel of cell populations that are related but have different abilities to shed metastases in inbred animals. Therefore, the differences in gene expression between the cell populations are likely to reflect mainly the differences in their metastatic potential. Second, the use of inbred rats for the model provides both a uniform genetic background, reducing the 'noise' in the

microarray data and readily the available tumour tissue. Third, the cells exhibit in vitro behaviours that can be related to their in vivo metastatic potential and offer opportunities for assaying in vitro the effects of genes revealed by the microarray. For example, in this model, changed morphology and increased speed of migration in vitro is associated with higher metastatic potential.

Our microarray analysis of the rat sarcoma model indicated that 23 genes were differentially expressed between metastatic and non-metastatic cells in a significant manner. One of these genes, *Epb41l3*, is significantly downregulated in metastasising sarcoma cells. *Epb41l3* was originally isolated as the cDNA DAL-1 from a screen of lung adenocarcinomas (Tran et al., 1999), which was later found to be a fragment of full-length *Epb41l3*. Its protein product 4.1B has an N-terminal FERM (4.1, ezrin, radixin, moesin) domain, a spectrin binding domain, a C-terminal domain, and the three unique domains U1, U2 and U3 (Parra et al., 1998). Like other members of the 4.1 family, 4.1B is thought to be involved in tethering the F-actin cytoskeleton to membrane proteins (Conboy, 1993). Its tumour suppressor activity has been demonstrated in lung adenocarcinoma, meningioma and breast carcinoma cell lines (Charboneau et al., 2002; Gutmann et al., 2001; Tran et al., 1999), and also as being lost in about 60% of lung adenocarcinomas (Tran et al., 1999) and meningiomas (Gutmann et al., 2000). Here, we show that 4.1B may also function as a metastasis suppressor by supporting orderly arrangements of actin stress fibres and suppressing the enhanced cell motility and chemotaxis associated with increased metastatic potential.

Results

Sarcoma model of metastasis developed in inbred LEWIS rats and the characterisation of four cell populations

We developed a rat sarcoma model of metastasis and analysed four related cell populations: K2, T15, A297 and A311 cells. To assess their metastatic potential, one-million cells were subcutaneously implanted into the back of inbred LEWIS rats. Primary tumours developed in all cases. Four to six weeks after the inoculation, metastases were found in the lungs of rats implanted with T15, A297 and A311 cells – with incidence shown in Fig. 1. The incidence of rats with metastases was significantly increased compared with the experimental group using K2 cells.

Since cell motility is thought to be critical at various points during the metastatic cascade, we studied the motile responses of the cells to a gradient of platelet-derived growth factor (PDGF) and insulin-like growth factor (IGF). The circular histograms in Fig. 2A present the distributions of the cell track directions and illustrate the differences in chemotaxis. K2 cells did not show a significant chemotactic response in this analysis. By contrast, the T15, A297 and A311 cells showed significant chemotactic responses (ANOVA $P<0.05$). There were also differences in the distribution of speed of cell migration (Fig. 2B). The non-metastatic K2 cells migrated at 11.1±0.5 μm/hour (mean ± s.e.m.), and the T15, A297 and A311 cells at 17.1±0.7 μm/hour, 19.1±0.9 μm/hour and 14.1±0.9 μm/hour respectively. The difference between K2 and T15 cells was statistically significant (ANOVA $P<0.05$). Similarly, the difference between A297 and K2 cells was

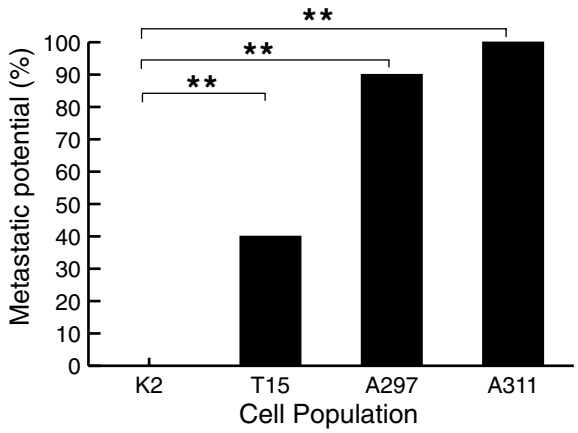

Fig. 1. Comparison of the metastatic potential among the sarcoma cell populations. Cell populations K2, T15, A297 and A311 were subcutaneously implanted (one-million cells per transplant), into inbred Lewis rats. Primary tumours developed in all cases. The metastatic potential – the percentage of subjects developing metastases – was calculated for each cell population. The K2 cells had no metastatic potential, whereas T15, A297 and A311 cells had metastatic potentials of 38%, 90% and 100%, respectively. The metastases were found in the lungs. The numbers of rats used to test the K2, T15, A297 and A311 cells were 20, 24, 10 and 10, respectively; χ^2 $^{**}P<0.01$.

statistically significant (ANOVA $P<0.01$). The difference in the speed of cell migration between A311 and K2 cells was not significant; however the fraction of cells migrating faster than 20 μm/hour was significantly larger (χ^2 $P<0.01$) in A311 cells (20%) compared with K2 cells (8%). We conclude that the speed of in vitro migration for the metastatic cells is increased, at least in a subpopulation of the cells. In the following experiments testing motility of treated cells in vitro we focused on K2 and T15 or A297 cells whose speed of cell migration was significantly changed between the whole populations.

We have shown previously that three cell populations (K2, T15 and A239/870N) from this model have distinct F-actin arrangements, and postulated that these were related to metastatic potential (Pokorna et al., 1994). Here, we have added two new cell populations with higher metastatic potential and re-evaluated the cell behaviour, in parallel to the microarray analysis, because cell characteristics may change through time. Indeed the A239/870N cells had reduced metastatic potential and were excluded from further study. Differences in F-actin organisation for the four populations included in this study – and presented in Fig. 3A – are consistent with the previous findings. The non-metastatic cells tend to have F-actin arranged into thick stress fibres that traverse the cell, whereas the metastatic cells are usually polarised, with their F-actin concentrated into ruffles at the leading edge, and elsewhere arranged cortically and in a disordered manner. Quantification of randomly acquired fields revealed that 89±8% of the non-metastatic K2 cells contained at least one stress fibre, in comparison to significantly ($P<0.001$) reduced levels in the metastatic T15, A297 and A311 cells, where the incidences of cells with stress fibres were 7±2%, 3±8% and 7±8%, respectively (Fig. 3B).

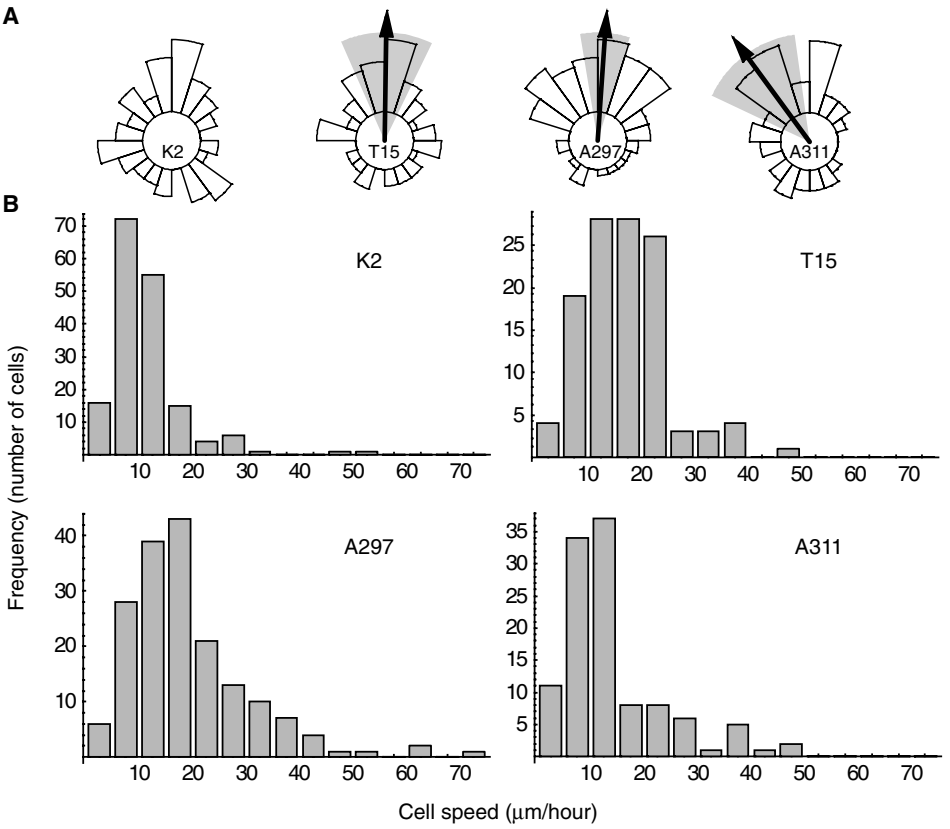

Fig. 2. Motile responses of the sarcoma cells to PDGF-IGF. (A) Distribution of directions of cell translocation in a gradient of PDGF-IGF in the Dunn chemotaxis chamber is represented by circular histograms. The circular histograms are aligned such that the concentration of PDGF-IGF in the gradient increases vertically towards the top. Translocation of a cell from its starting point was evaluated and its direction was taken on migrating 70 μm. Cells not migrating 70 μm were not included in this analysis. Significant unimodal clustering of directions according to the Rayleigh test is indicated by an arrow identifying the mean direction, and a shaded wedge representing its 95% confidence interval. K2 cells are weakly chemotactic to PDGF-IGF, whereas T15, A297 and A311 cells have strong chemotactic responses (P<0.005). Data from left to right are from K2, T15, A297 and A311 cells and represent 5, 4, 5 and 5 independent experiments, respectively, each recorded over a period of 16 hours. The total numbers (fractions) of K2, T15, A297 and A311 cells included in the analysis are 61 (36%), 81 (70%), 86 (49%) and 47 (42%), respectively. (B) Histograms to illustrate the distribution of speed of cell migration within the four cell populations. The non-metastatic K2 cells moved at 11.1±0.5 μm/hour, whereas the metastatic T15 and A297 cells moved significantly faster,at 17.1±0.7 μm/hour (ANOVA P<0.05) and 19.1±0.9 μm/hour (ANOVA P<0.01), respectively. There was no significant difference between the speed of cell migration in K2 and A311 cells, which migrated at 14.1±0.9 μm/hour. However, the proportion of cells moving faster than 20 μm/hour was significantly increased (χ^2 P<0.01) in A311 cells (20%) compared with K2 cells (8%). The speed data were also derived from the experiments with the Dunn chemotaxis chamber without excluding any cells. The total numbers of K2, T15, A297 and A311 cells were 171, 116, 176 and 113, respectively, and numbers of 5-minute displacements were 21340, 13390, 20179 and 15436, respectively.

Microarray analysis of the sarcoma cell populations reveals genes with a potential role in metastasis

To investigate the gene expression differences underlying the differences in metastatic potential, the F-actin cytoskeleton and motility, we performed microarray analysis of the cultured cells and the tumours that arose when the cells were implanted into rats. We subjected the cultured cells to three treatments: (1) starvation in 0.5% serum for 5 hours, (2) 5-hour starvation followed by 30-minute treatment with PDGF-IGF and (3) 5-hour starvation followed by a 3-hour treatment with PDGF-IGF. These regimens reflect the times in the Dunn chemotaxis assay at which cell motility is low, commencing, and at its peak. Our analysis showed that treatment with PDGF-IGF did not have any significant effect on gene expression (P>0.08 for all individual changes). Therefore, the gene expression values of the treatments were averaged to obtain the gene expression value for each cell population. We then looked for significant (P<0.05) differences in gene expression, more than 2.5 times in the non-metastatic and metastatic cell populations. Additionally, we rejected genes whose expression did not correlate between the cultured cells and primary tumours, thus restricting our investigations to genes whose expression is regulated in vitro in the same way as in vivo. This procedure generated a list of twenty-three candidate genes (Table 1). To validate the microarray data, we performed reverse transcriptase (RT)-PCR for ten of the candidate genes and observed the same expression patterns as those seen in the microarray (Fig. 4). We then started analysing the functional effects of identified genes. Cell cytoskeleton-related proteins were given a priority when we were choosing the candidates. We selected *Bk*, *Cask*, *Epb41l3* and *Ril*, and found that overexpression or knockdown of *Bk*, *Cask* and *Ril* had no noticeable effect on the motility, cytoskeleton or morphology of the sarcoma cells in vitro. However, our studies indicated a role for *Epb41l3* in F-actin organisation and cell motility.

Expression and localisation of 4.1B protein, the product of *Epb41l3* gene

The expression of *Epb41l3*, which encodes the protein 4.1B, is significantly reduced 36 times in the metastatic sarcoma cells (Fig. 5A). The similarity of expression patterns in the cultured cells and the primary tumours excludes the possibility that the differential expression of *Epb41l3* is owing to cell culture conditions alone. The transcription data were confirmed at the protein level by western blotting (Fig. 5B) by which 4.1B protein was undetectable in the metastatic cells. While cloning rat *Epb41l3*, we unexpectedly found a third splice variant (GenBank accession number DQ462202, shown in

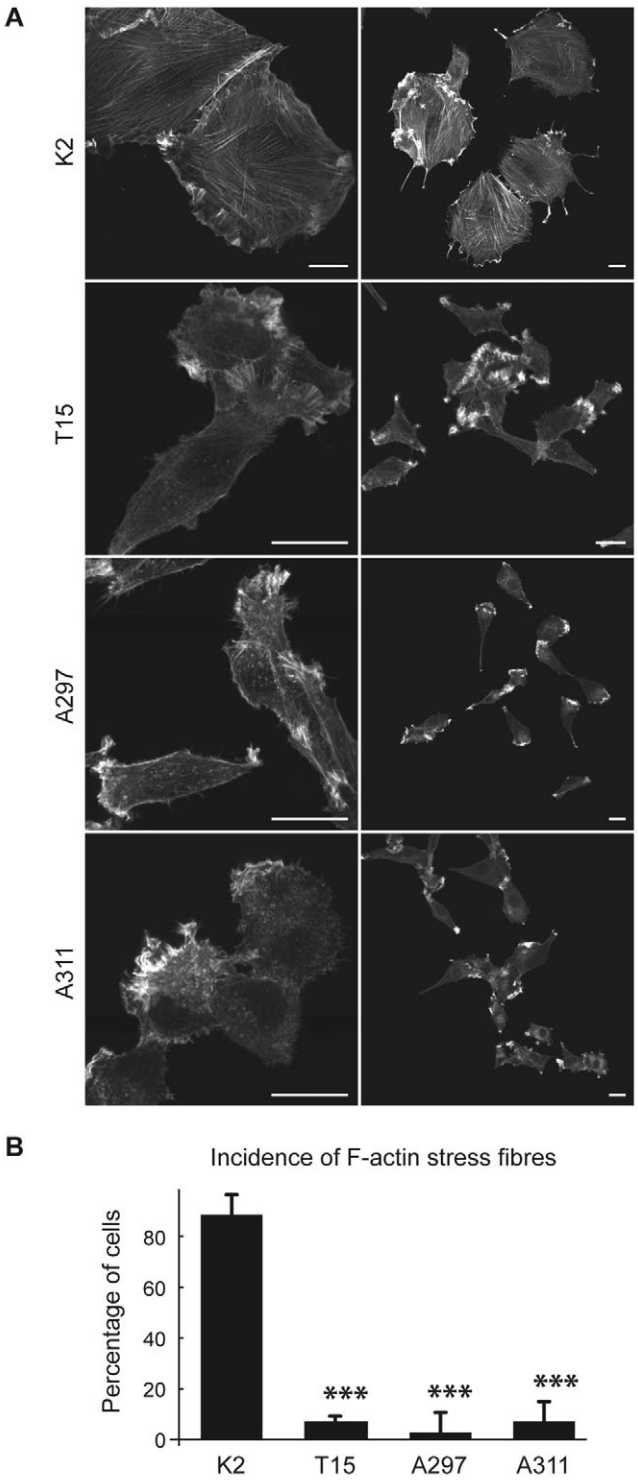

Fig. 3. Differences in F-actin organisation among the sarcoma cell populations. (A) These single confocal images of Rhodamine-phalloidin-stained cells reveal differences among the sarcoma cell populations. Lower magnification images (right panels) demonstrate that these phenotypes are representative across a larger number of cells. F-actin in K2 (non-metastatic cells) is arranged into stress fibres, which can be quite thick and can traverse the cell. T15, A297 and A311 cells typically have F-actin concentrated into ruffles at the leading edge of the cell; elsewhere it is arranged cortically and in a disordered manner. These cells are often polarised. Bars, 20 μm. (B) The percentage of actin stress fibre-containing cells in each population. Quantification of randomly acquired fields of cells revealed that 89±8% of K2 cells contain at least one stress fibre, compared with only 7±2%, 3±8% and 7±8% of T15, A297 and A311 cells, respectively. The numbers of cells scored for K2, T15, A297 and A311 were 34, 84, 58 and 69, respectively. The individual differences in stress fibre distribution between the T15, A297 and A311 compared with K2 cells are all significant (***P<0.001).

supplementary material Fig. S2). The localisation of 4.1B was investigated using a GFP fusion protein. In sarcoma and HeLa cells, GFP-4.1B is cytoplasmic and excluded from the nucleus (Fig. 6). There is colocalisation with F-actin, particularly in areas of apparent protrusive activity (Fig. 6G,H). It is also enriched at the plasma membrane (Fig. 6I,L). This localisation pattern matches closely immunocytochemical analysis of NCI-460 cells (Tran et al., 1999) and MCF-7 cells (Charboneau et al., 2002). Therefore we conclude that the GFP-4.1B fusion protein adequately reflects the true localisation of the endogenous 4.1B protein. We also identified enrichments of GFP-4.1B localised in many but not all focal adhesions, visualised using interference reflection microscopy, in T15 sarcoma cells (Fig. 7).

Downregulation of 4.1B causes a loss of actin stress fibres

We observed that the depletion of 4.1B from K2 cells by treatment with siRNA targeting *Epb41l3* leads to an altered F-actin cytoskeleton (Fig. 8A). The control cells and uninjected cells are characterised by thick stress fibres, whereas the *Epb41l3* siRNA-treated cells have fewer stress fibres and less total F-actin. Such an arrangement of F-actin is typical of the metastatic cell populations (see Fig. 3). To quantify the effect of *Epb41l3* siRNA on stress fibres, it was necessary to analyse a large number of cells. Therefore, we performed these experiments in HeLa cells, which are more amenable to chemical transfection, rather than the sarcoma cells. Fig. 8B shows that siRNA targeting human *EPB41L3* causes a loss of actin stress fibres, and an overall reduction of F-actin in HeLa cells. Western blotting (Fig. 8C) confirmed that 4.1B is expressed in HeLa cells and that its expression can be reduced by treatment with *EPB41L3* siRNA. To be certain that the loss of stress fibres is due to the silencing of *EPB41L3* and not because of an unspecific effect of the siRNA, we performed an RNA interference (RNAi) rescue experiment. Fig. 8D shows confocal images of cells that were transfected with *EPB41L3* siRNA followed by RNAi-resistent 4.1B cDNA or GFP cDNA 48 hours later. The cells expressing RNAi-resistent 4.1B recovered their typical F-actin morphology, whereas the cells transfected with GFP as a control maintained the phenotype of a disrupted F-actin cytoskeleton. Quantification of the confocal images (Fig. 8E) revealed that, when transfected with control siRNA, stress-fibre-containing HeLa cells typically comprised just over 50% of the population. However, when the cells were transfected with *EPB41L3* siRNA, the percentage of actin stress-fibre-containing cells significantly decreased to under 25%, irrespective of absence or presence of subsequent GFP expression. In the RNAi-rescue cells, the percentage of cells with F-stress fibres recovers to a level that is not significantly different from the cells transfected with control siRNA. Therefore, we are confident that the effect on the F-actin

Table 1. Genes differentially expressed between metastatic and non-metastatic cell populations

Gene description	Gene ontology	Relative expression level
Gremlin 1 homolog (*Grem1*)	Cell-cell signalling; embryonic patterning; organ morphogenesis	0.006
PAR-related orphan receptor alpha, Rora_predicted	Transcriptional regulation; DNA-dependent signal transduction	0.027
Erythrocyte protein band 4.1-like 3 (*Epb41l3*)	Cell proliferation; cortical actin cytoskeleton; actin organisation	0.028
Ca/CaM-dependent serine protein kinase (*Cask*)	Protein complex assembly; protein phosphorylation; transport	0.031
Hypothetical gene AF152002, LOC290595		0.063
EST, Affymetrix Identifier 1376071_at		0.069
Polo-like kinase 2 (*Plk2*)	Protein phosphorylation; cell cycle	0.080
EST, Affymetrix Identifier 1375986_at		0.14
RNase A family 4 (*Rnase4*)	mRNA cleavage	0.15
Similar to CG12279-PA, LOC500420		0.17
Translin-associated factor X (*Tsnax*)		0.18
A disintegrin-like and metalloproteinase (*Adamts1*)	Proteolysis; integrin signalling; cell proliferation	0.22
Growth differentiation factor 1, Gdf1_predicted		0.25
EST, Affymetrix Identifier 1391428_at		0.25
Neogenin (*Neo1*)	Protein phosphorylation; cell motility; cell adhesion	0.29
Similar to RIKEN cDNA 9330161F08, LOC362899		3.0
Reversion-induced LIM gene (*Ril*)	Intracellular signalling; actin cytoskeleton organisation	4.5
Brain and kidney protein, LOC497736 (*Bk*)	Transport; cAMP-mediated signalling	4.6
EST; affymetrix identifier 1373642_at		5.1
EST; affymetrix identifier 1377065_at		5.8
Ankyrin 3, epithelial isoform g, RGD:620157 (*Ank3*)	Signal transduction; positive regulation of apoptosis	12.2
Similar to synaptopodin-2, LOC499702		17.1
Chondroitin sulfate proteoglycan 4 (*Cspg4*)	MAPK activation; cell motility; cell adhesion	65.1

Expression levels in the three metastasising cell populations from tissue culture and primary tumours were divided by expression levels in the non-metastasising cell population from tissue culture and primary tumours, producing six relative expression levels for each tested gene. To produce this list of 23 candidate genes, we selected genes that have the six relative expression levels of >2.5 or <0.4; also, the relevant difference in the expression had to be significant (P<0.05). Given are the averages of the six individual relative expression levels for each candidate gene.

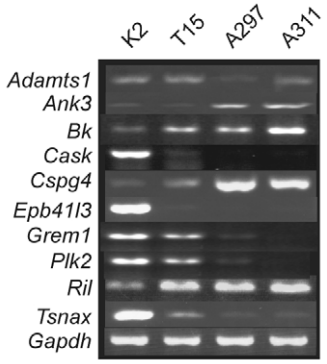

Fig. 4. RT-PCR was performed for ten of the candidate genes to validate the microarray data. PCR products were resolved on a 1% TBE agarose gel supplemented with ethidium bromide, and visualized by UV trans-illumination. We observed the expression patterns that had been indicated by the microarray. *Gapdh* was used as control and was expressed uniformly.

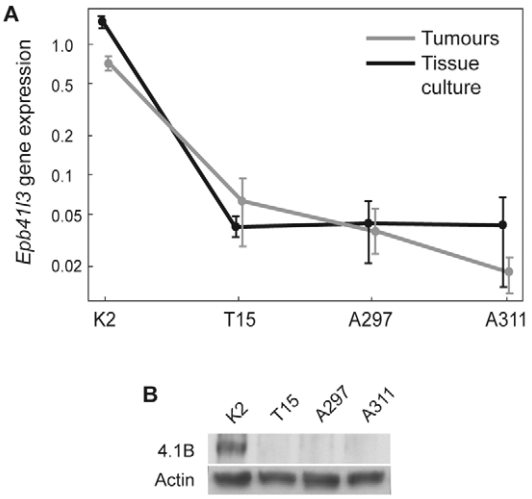

Fig. 5. Expression of *Epb41l3,* encoding 4.1B protein, in the sarcoma cells. (A) Normalised expression levels of the *Epb41l3* gene are shown for the cultured cells and the primary tumours. The normalisation was based on median values from individual microarrays. Each dot and bar represents the mean value ± s.e.m. of the expression levels obtained from multiple microarrays. *Epb41l3* is significantly downregulated in the metastatic cells (P<0.05), and this expression pattern is closely matched by that of the tumours. (B) The difference in expression also occurs at the protein level, as seen in this western blot, in which very little 4.1B is detectable in cultured T15, A297 and A311 cells. Actin was used as a loading control.

cytoskeleton is specifically due to the decrease in 4.1B. Having controlled for potential adverse effects of microinjection in K2 cells by including a GFP control and having performed rescue experiments to test for possible adverse consequences of chemical transfection in HeLa cells, we conclude that the 4.1B siRNA treatment causes loss of stress fibres in HeLa cells as well as in the sarcoma cells.

The effect of 4.1B expression on cell motility and chemotaxis

We investigated the function of 4.1B in cell motility by using siRNA to reduce its expression in non-metastatic K2 cells and cDNA to express it in metastatic T15 cells. K2 cells treated with *Epb41l3* siRNA significantly increased speed, migrating about twice as fast (Fig. 9A) compared with those injected

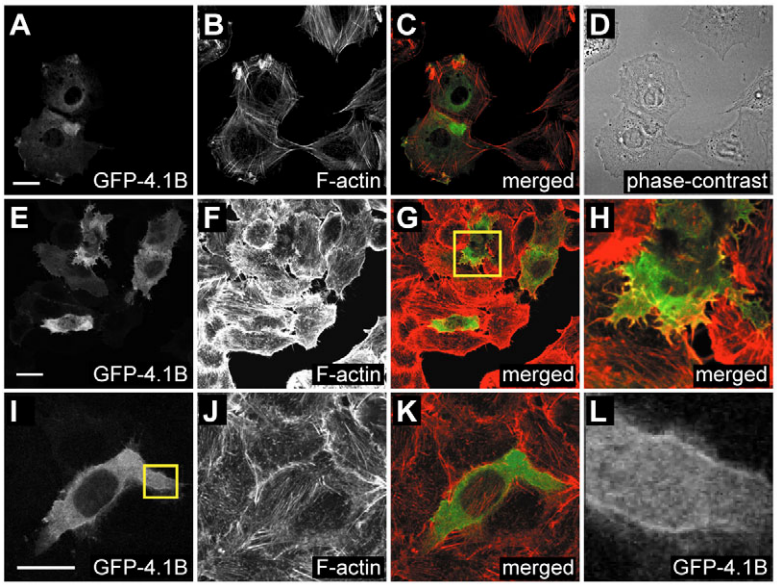

Fig. 6. Cellular localisation of GFP-4.1B fusion protein. To investigate the localisation of 4.1B, cells were transfected with GFP-4.1B fusion construct and, 24 hours later, fixed and stained with Rhodamine-phalloidin. (A-D) Sarcoma cells K2. (E-L) HeLa cells. (A) GFP-4.1B is expressed in the cytoplasm and is enriched at the plasma membrane. (B,C) There is also some colocalisation with F-actin especially at the plasma membrane compartment enriched with GFP-4.1B. The brighter area of GFP-4.1B between the two cells in A is probably a result of the two cells overlapping, suggested by the phase-contrast image (D). (E,F) Localisation of 4.1B in HeLa cells is similar, with cytoplasmic expression and some colocalisation with F-actin (G), especially in peripheral areas of ruffling and protrusive activity, as seen in the enlarged region (H; boxed region in G). There is also an enrichment of GFP-4.1B at the membrane (I-K). This is clearer still in the close-up (L) of the boxed region in (I). All images are single confocal images and representative of three independent experiments. Bar, 20 μm.

with control siRNA (ANOVA $P<0.01$). The same experiment was performed as a control in A297 cells, which do not express 4.1B. There was no change in cell migration (no significance in ANOVA, mean ± s.e.m. of normalised speed of cell migration 1.3±0.1 and 1.0±0.1 for control siRNA and *Epb41l3* siRNA, respectively; a total of 20 cells from five time-lapse experiments was analysed) which supported the specificity of the siRNA effect on speed of cell migration. Having seen an increase in speed of cell migration in 4.1B-depleted K2 cells, we performed the complementary experiment by overexpressing 4.1B cDNA in T15 cells, which do not endogenously express detectable levels of 4.1B. Cells were microinjected – with GFP cDNA alone or a mixture of 4.1B and GFP cDNA – and analysis of their movements revealed significant differences in speed of cell migration. The expression of 4.1B caused a reduction in cell motility; cells injected with 4.1B and GFP cDNA migrated at approximately half the speed (Fig. 9B) of those injected with GFP cDNA (ANOVA $P<0.01$). We also evaluated chemotaxis of the metastatic T15 cells exogenously expressing 4.1B and found that the treatment significantly (ANOVA $P<0.05$) reduced the chemotactic response (Fig. 10); the speed of cell migration was also significantly reduced (ANOVA $P<0.02$).

Discussion

Here, we have described the use of a rat sarcoma cell model to identify a potential metastasis suppressor protein, 4.1B. These rat sarcoma cells exhibited in vitro behaviour that can be related to their metastatic potential. First, the cells had significantly different arrangements of F-actin, which could influence their metastatic potential because cytoskeletal regulation is a key determinant of invasion. Second, the metastatic cells showed increased chemotaxis towards PDGF-IGF; chemotaxis towards blood vessels might be important during intravasation (Wyckoff et al., 2000). Last, the metastatic cell populations contained a larger subpopulation of fast-migrating cells. Enhanced cell motility is a common feature of metastatic cells and has been described by several groups. A recent in vivo study has shown that metastatic tumour cells move 4.5 times as frequently as non-metastatic tumour cells in the same tumour microenvironment (Sahai et al., 2005). It has been suggested that only a subpopulation of cells from a tumour, rather than every cell in the tumour, becomes metastatic (Fidler and Hart, 1982). Therefore, it is reasonable to suppose that the increased speed of migration of these subpopulations contributes to the increased metastatic potentials observed in T15, A297 and A311 cells.

Our model has advantages for the microarray study of metastasis, because the cell populations originated from a common, spontaneous tumour transformation, and were unlikely to show the genetic heterogeneity that can complicate the interpretation of microarray data. The use of inbred rats further helped to reduce heterogeneity. Thus, we were able to focus on the genetic differences contributing to the different abilities of cell populations and tumours to shed metastases. Indeed, we found relatively few differentially expressed genes.

We had included a growth factor treatment in the microarray experiment because, in our model, progression to the invasive phenotype correlated with enhanced chemotaxis to a gradient of PDGF-IGF. We found that an up to 3-hour treatment with PDGF-IGF had no significant effect on gene expression. A possible explanation for this is that a short treatment with PDGF-IGF may exert its effect via molecular switches, whose activation state cannot be determined by microarray analysis. We took advantage of the unchanged gene expression by averaging the mean expression values for the three growth factor treatments, which improved the statistical significance of the data.

The reliability of our microarray data is demonstrated in two ways. First, RT-PCR of ten candidate genes confirmed the expression patterns found by the microarray analysis. Second, some of the genes identified, for example, *Cspg4*, *Ankyrin 3*, *Grem1* and *Neo1*, have already been implicated in metastasis by other groups. Moreover, we have shown functional effects for one of the candidate genes. Of the 23 most differentially expressed genes, 15 are downregulated and eight are upregulated in metastasis. *Cspg4*, coding for the proteoglycan NG2, is overexpressed approximately 65 times in metastatic

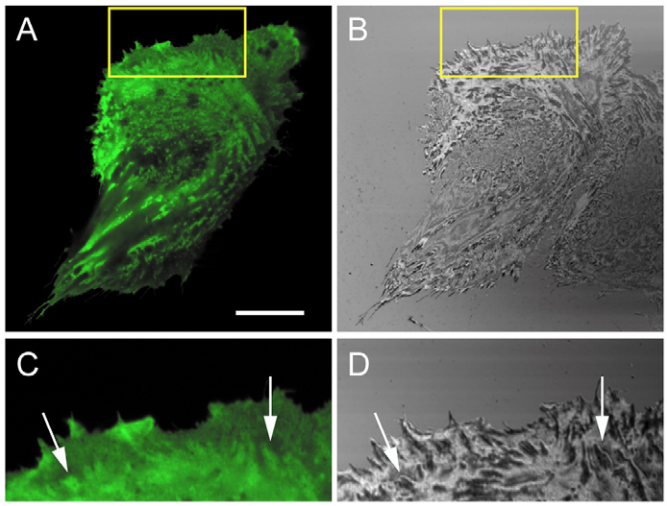

Fig. 7. Distribution of GFP-4.1B and focal adhesions in a T15 cell. The cell was microinjected with GFP-4.1B fusion construct, fixed after 5 hours and analysed under a laser scanning confocal microscope. (A-D) We simultaneously acquired an image of GFP-4.1B at the substrate level (A) and an interference reflection microscopy image (B) in which focal adhesions appear dark. C and D are enlarged images of boxed regions in A and B, respectively. They reveal enrichment of GFP-4.1B in many but not all focal adhesions. Arrows indicate examples of focal adhesions with an increased concentration of GFP-4.1B. Bar, 20 μm.

cells. Burg et al. reported that expression of NG2 in melanoma cells enhanced their metastatic properties (Burg et al., 1998). Ankyrin 3, which binds the Rho guanine-nucleotide exchange factor Tiam1, is upregulated approximately 12 times in the metastatic cells. Bourguignon et al. report that the Tiam1/Ankyrin interaction promotes Rac1 signalling and migration in SP1 mouse breast tumour cells (Bourguignon et al., 2000). The function of Tiam1 is likely to be affected by an increased availability of ankyrin, such as in the metastatic cells of this model. Reversion-induced LIM protein (RIL) is overexpressed with metastasis. RIL may be a regulator of actin stress fibre turnover because Vallenius et al. (Vallenius et al., 2004) found that expression of RIL caused the rapid formation of new stress fibres and frequent collapse of thick stress fibres. A dynamic actin cytoskeleton is essential for cell motility and metastasis and, therefore, the increased availability of a regulator of actin turnover such as RIL would be an advantage to a metastasising cell. *Grem1*, encoding gremlin, a negative regulator of monocyte chemotaxis (Chen et al., 2004), is downregulated with metastasis. This could explain the strong chemotaxis to PDGF-IGF and enhanced motility in our metastasising cells. Gremlin can also suppress transformation and tumorigenesis (Topol et al., 1997) so its upregulation in the non-metastatic cells might prevent their successful growth in a new site and account in part for their inability to cause metastases. The metalloprotease ADAMTS-1 is downregulated with metastasis in our model which agrees with Kuno et al., who reported that overexpression of ADAMTS-1 in CHO cells causes the inhibition of tumour growth and metastasis (Kuno et al., 2004). Plk2 was significantly downregulated in our metastasising cells and a similar downregulation mediated by transcriptional silencing in malignant lymphomas was reported by Syed et al. (Syed et al., 2006). They also showed that the Plk2 expression promoted apoptosis, which might also be important in our sarcomas. Although there is currently no clear role for RNase 4 in cancer, there are instances where unusual RNase levels have been detected in cancer patients (Peracaula et al., 2000) and RNase 4 was downregulated in our metastasising sarcoma cells. Neogenin, which is downregulated in our metastatic cells, might play a role in mammary carcinogenesis, because its expression is inversely correlated with mammary carcinogenicity (Lee et al., 2005), which again supports the pattern of expression we report here.

The main focus of this study is the protein 4.1B. Our data suggest that 4.1B functions as a metastasis suppressor because its loss supports a reorganisation of the F-actin cytoskeleton and concomitant enhanced cell motility, both of which are likely to be important in metastasis. 4.1B has not previously been related to the development of metastasis, but the tumour suppressor activity of 4.1B has been demonstrated in several cell lines and 4.1B loss reported in various cancers (Charboneau et al., 2002; Gutmann et al., 2001; Kikuchi et al., 2006; Tran et al., 1999). We found that the *Epb41l3* transcript in the sarcoma cells is a variant of the 4.1B minor isoform type II, and therefore represents a third splice variant of *Epb41l3*. Different splice variants of *Epb41l3* are thought to contribute to its tissue specificity (Gascard et al., 2004).

Depletion of 4.1B in K2 sarcoma cells by a specific siRNA resulting in a loss of stress fibres was also observed in HeLa cells treated with three independent siRNAs, which demonstrates that this response is more general and not restricted to our sarcoma model. A reduction in stress fibres that accompany the metastatic phenotype has been also observed by others (Khanna et al., 2001). The relationship between 4.1B and the F-actin cytoskeleton was further explored by expressing 4.1B in the metastatic cells. The exogenous expression of 4.1B in metastatic T15 cells, which have no endogenous expression, was without an apparent effect on F-actin organisation (data not shown). We conclude that 4.1B in the non-metastatic K2 cells is necessary for the presence of actin stress fibres, whereas the exogenous expression of 4.1B in the metastatic cells is not sufficient for the reappearance of stress fibres; most likely, additional changes in expression are required.

We also found that reduction of 4.1B expression in non-metastatic K2 cells by siRNA treatment caused speed of cell migration to double. Correspondingly, exogenous expression of 4.1B in the metastatic T15 cells reduced their speed approximately by half and, additionally, significantly suppressed chemotaxis. The fact that overexpression of 4.1B, and also its depletion, can lead to changes in motility in different cell types, strongly suggests that 4.1B is important for cell migration in this model. Furthermore, F-actin rearrangements that accompany changes in speed of cell migration have been observed by others. For example, Clark et al. reported that metastatic cells migrate more and have more filopodial protrusions than cells from primary tumours (Clark et al., 2000). We conclude that the experimental reduction of 4.1B expression by RNAi in non-metastasising cells, which mimicks the loss of 4.1B in the metastatic cells, induces a reduction of stress fibre occurrence, and enhanced cell motility and chemotaxis thus introducing important aspects of the metastatic phenotype in the

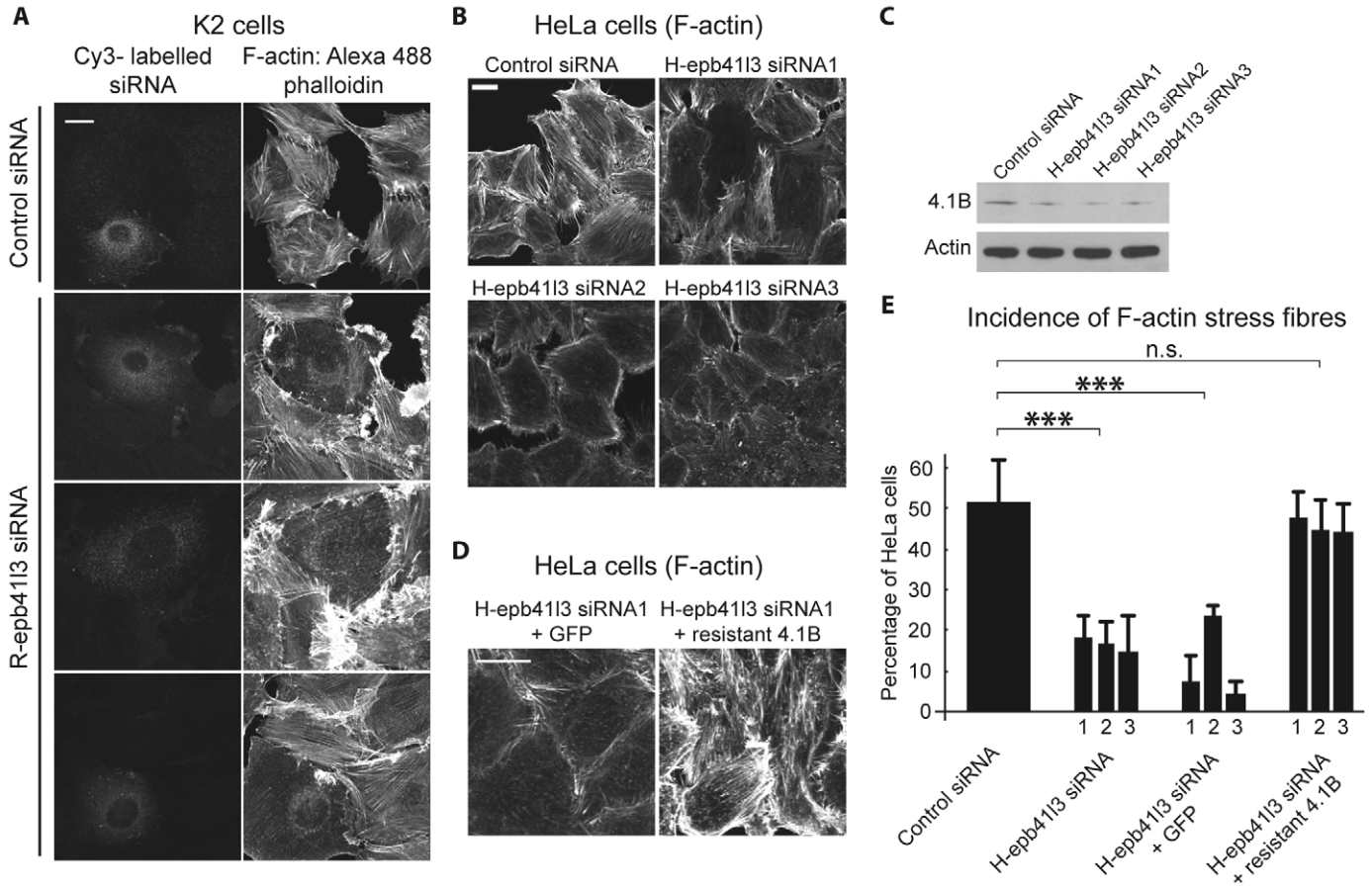

Fig. 8. Depletion of 4.1B by RNAi causes disruption of the F-actin cytoskeleton. (A) K2 cells injected with Cy3-labelled siRNA targeting rat *Epb41l3* (R-epb41l3 siRNA) or control siRNA were fixed 48 hours later and labelled with Alexa Fluor-488–phalloidin. Cells with siRNA targeting rat *Epb41l3* displayed a disrupted F-actin cytoskeleton, with fewer stress fibres and less total F-actin. Cells transfected with Cy3-labelled control siRNA were unchanged. (B) Similarly, HeLa cells transfected with three independent siRNAs targeting human *EPB41L3* (H-epb41l3 siRNA1, H-epb41l3 siRNA2 and H-epb41l3 siRNA 3) exhibited fewer stress fibres after 48 hours of incubation. Some fine stress fibres remained, but the majority of cells had a disordered F-actin cytoskeleton and few F-actin; images are representative of five independent experiments. F-actin was labelled with Rhodamine-phalloidin. (C) Western blot confirming that HeLa cells transfected with three independent siRNAs targeting human *EPB41L3* expressed reduced levels of 4.1B after 48 hours. Densitometric quantification showed that the actin-normalised presence of 4.1B was reduced to 44%, 18% and 28% when using H-epb41l3 siRNA1, H-epb41l3 siRNA2 and H-epb41l3 siRNA3, respectivley. (D) *EPB41L3* siRNA-treated HeLa cells transfected with GFP cDNA as a control exhibited lack of stress fibres similarly to the experiments with siRNA on its own shown in B. *EPB41L3* siRNA-treated HeLa cells subsequently transfected with an RNAi-resistant 4.1B cDNA recovered stress fibres and organised F-actin structures to similar levels observed in control siRNA treated cells shown in B. This rescue experiment confirms that the siRNAs were specific; images shown in D are representative of three independent experiments. F-actin was labelled with Rhodamine-phalloidin. (E) Quantitative analysis of HeLa cells with actin stress fibres showed that siRNA targeting human *EPB41L3* resulted in a significant reduction, from half of the cells to less then a quarter on average (ANOVA ***P<0.001; the numbers of cells evaluated for control siRNA were 48 and 427 for siRNA targeting human *EPB41L3*). *EPB41L3* siRNA-treated HeLa cells with and without GFP cDNA transfection had similar significantly reduced numbers of cells with actin stress fibres (ANOVA ***P<0.001; 216 siRNA-treated cells transfected with GFP cDNA were evaluated). *EPB41L3* siRNA-treated HeLa cells transfected with an RNAi-resistant 4.1B cDNA did not have significantly changed number of cells with actin stress fibres compared with the control siRNA (n.s., no significance in ANOVA; 766 siRNA-treated cells transfected with RNAi-resistant 4.1B cDNA were evaluated). Cells that lost actin stress fibres exhibited disordered F-actin, with F-actin puncta and cortical F-actin organisation.

non-metastatic cells. Although the metastasising sarcoma cells show an increasing trend in the metastatic potential, we did not see a similar tendency in changes of stress fibre morphology, cell motility or 4.1B expression. It is likely that these changes represent an important step in tumour progression towards a metastatic phenotype common to all three metastasising populations, and additional changes are required to increase the metastatic potential further.

We found that GFP-4.1B was expressed at cell-cell contacts in the sarcoma cells and at the plasma membrane, which agrees with data from other groups (Tran et al., 1999; Charboneau et al., 2002). 4.1 proteins are known to tether the cytoskeleton to the membrane by crosslinking spectrin and/or actin dimers to integral membrane proteins (Conboy, 1993). Therefore, we propose that the loss of stress fibres and enhanced motility is mediated by the role of 4.1B in linking F-actin to focal

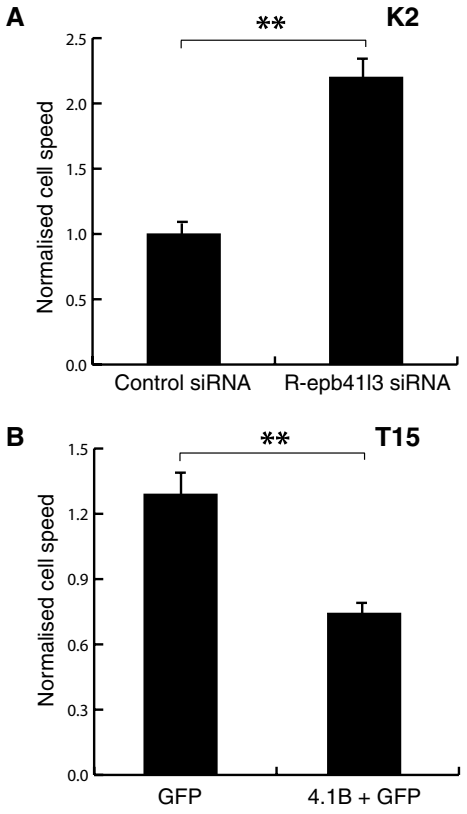

Fig. 9. Effect of 4.1B on the motility of the sarcoma cells. (A) Non-metastatic K2 cells were injected with Cy3-labelled R-epb41l3 siRNA1 and recorded 48 hours later by low light level digital microscopy. Cell translocations were interactively tracked, and speeds of cell migration evaluated in Mathematica. Speed of cell migration was increased twofold in cells treated with siRNA targeting epb41l3 compared with those treated with control siRNA (ANOVA $P<0.01$; mean ± s.e.m. of normalised speed of cell migration was 1.0±0.1 and 2.2±0.2 for control siRNA and siRNA targeting *Epb41l3*, respectively; a total of 49 cells from ten time-lapse recordings was analysed). (B) GFP cDNA, or a mixture of GFP and 4.1B cDNA, were microinjected into metastatic T15 cells and after 5 hours cell movements recorded by low light level digital microscopy. Cells expressing both 4.1B and GFP migrated at half the speed of the cells injected with GFP alone (ANOVA $P<0.01$; mean ± s.e.m. of normalised speed of cell migration was 1.3±0.1 and 0.7±0.1 for GFP cDNA alone and for mixture of GFP and 4.1B cDNA, respectively; a total of 49 cells from nine time-lapse recordings was analysed).

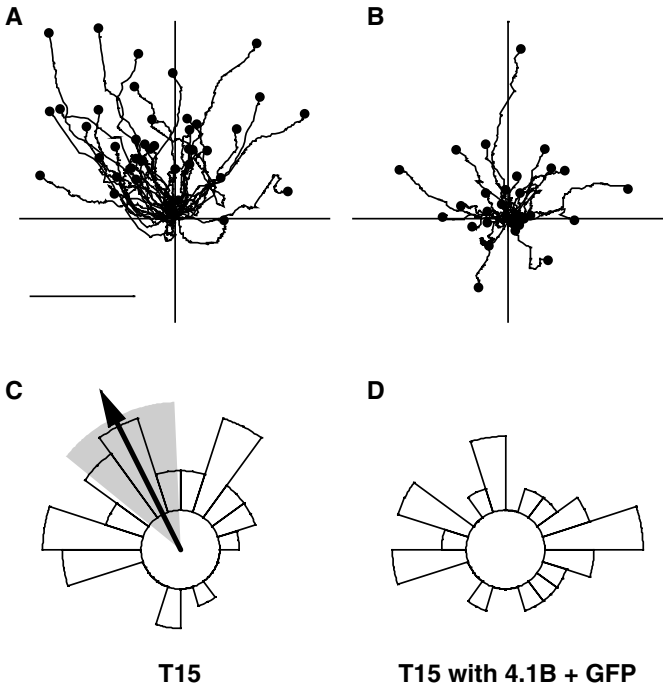

Fig. 10. Effect of exogenous 4.1B expression on the chemotaxis of T15 sarcoma cells. The motility of cells in the Dunn chemotaxis chamber was recorded 5 hours after microinjection and evaluated in a way similar to experiments presented in Fig. 2A. (A,B) Cell tracks with starting points shifted to a common origin are for uninjected cells (A) and in cells expressing a mixture of 4.1B and GFP (B). Bar, 100 μm. The speed of cell migration of the expressing cells was significantly reduced 2.3 times (ANOVA $P<0.02$; numbers of time-lapse recordings and cells were 14 and 41, respectively, for uninjected cells, and 9 and 29, respectively, for cells expressing 4.1B and GFP). (C,D) Circular histograms of cells that migrated 10 μm for uninjected cells (C) and for cells expressing 4.1B and GFP (D). Arrow (mean direction) and a grey wedge (its 95% confidence interval) indicate unimodal significant clustering of the directions (Rayleigh test $P<0.001$). The chemotactic response, measured by the displacement in the gradient direction, is significantly different (ANOVA $P<0.05$; numbers of cells that migrated 10 μm were 41 for uninjected cells and 27 for cells expressing 4.1B and GFP).

adhesions and plasma membrane. Our finding of GFP-4.1B enrichment in many focal adhesions supports this possibility.

Recent clinical data provide further support for the relevance of our findings to metastasis. The profiling database Oncomine™ (www.oncomine.org) presents an example of significant downregulation of 4.1B protein in human metastatic, infiltrating lobular carcinoma of breast, using all secondary sites in comparison to the primary tumour. Three probes of *EPB41L3* expression were used and the changes in expression levels were between 0.32 and 0.60 times, with *P* values between 0.007 and 0.031. Another example, the loss of heterozygosity of the region of chromosome 18, where *EPB41L3* is localized, has been observed in more than 55% of invasive ductal carcinoma in situ (DCIS) tumours (Kittiniyom et al., 2001). The epigenetic inactivation of *EPB41L3* by promoter methylation was found to be an indicator of poor prognosis in patients with lung adenocarcinoma (Kikuchi et al., 2005). Similarly, epigenetic inactivation of *EPB41L3* by promoter methylation was found to correlate with a shorter survival in patients with renal clear cell carcinoma (Kikuchi et al., 2006). These observations support our data, which suggest that the loss of 4.1B can enhance cell behaviours that are associated with metastatic potential.

In summary, we used a sarcoma model of metastasis to identify genes potentially associated with metastasis. We found some genes whose role in metastatic disease was already described, and others whose association in metastasis is as yet unconfirmed. Having studied one such gene, *Epb41l3*, we conclude that the loss of 4.1B protein in metastatic cells causes a loss of actin stress fibres and a significant increase in cell motility and, thus, plays a role in the progression to the metastatic phenotype.

Materials and Methods

Cell culture

K2 cells (full name LW13K2), are spontaneously transformed rat embryonic fibroblasts (Vesely and Weiss, 1973). T15 cells (full name RPSL4T15) were developed from K2 cells by neoplastic progression in vivo and in vitro (Vesely et al., 1987). A297 cells (full name A297Nb) were taken from a metastasis that formed in a rat injected with T15 cells. A311 cells (full name A337/311RP) were obtained from a metastasis that arose in a rat injected with the A297 cells. K2, T15, A297 and A311 cells were maintained in MEM with Hank's salts supplemented with 10% bovine serum (SML, Germany), 0.09% sodium bicarbonate, 0.12 g/l Na-pyruvate (Sigma) and 1 mM glutamine, at 37°C with 5% CO_2. HeLa cells were maintained in E4 medium supplemented with 10% foetal calf serum, at 37°C with 10% CO_2.

Assessment of metastatic potential

Cell populations were implanted subcutaneously into the back of Lewis rats at one-million cells per transplant. Animals were sacrificed 4-6 weeks later and dissected. All organs in the thoracic and abdominal cavities were carefully inspected for metastases. The metastatic potential is the percentage of rats developing metastases.

Low light level digital imaging microscopy, and analysis of cell motility and chemotaxis

Chemotaxis in a concentration gradient of 60 ng/ml PDGF and 80 ng/ml insulin-like growth factor (IGF) was assessed using the Dunn chemotaxis chamber as described previously (Zicha et al., 1991). To assess serum-stimulated random motility of cells with reduced 4.1B expression or exogenous 4.1B expression, we microinjected K2 or T15 cells that had been seeded on coverslips, with 2 μM Cy3-labelled siRNA targeting *Epb41l3*, or 0.075 μg/μl 4.1B cDNA construct mixed with GFP cDNA construct. Controls were 2 μM Cy3-labelled control siRNA or 0.05 μg/μl GFP cDNA construct alone. Cells treated with siRNA were incubated for 48 hours. Cells microinjected with the mixture of expression constructs were incubated for 5 hours. In both cases, the cells were then starved in medium containing reduced (0.5%) bovine serum for 5 hours, and assembled into chambers for live imaging in medium containing 10% bovine serum. In experiments assessing chemotaxis of T15 cells exogenously expressing 4.1B, we microinjected T15 cells on coverslips with a mixture of 4.1B and GFP contructs, starved the cells in 0.5% bovine serum for five hours and started time-lapse recording in the Dunn chamber. Movies were acquired using a 10× NA 0.32 phase-contrast objective on an Axiovert 135TV microscope (Zeiss) equipped with a Hamamatsu Orca ER CCD camera. AQM software (Kinetic Imaging) was used to capture one frame every 5 minutes for 16 hours. Cell translocations were interactively tracked using Motion Analysis software (Kinetic Imaging). Speed of cell migration and chemotaxis of the cells was evaluated using an algorithm implemented in Mathematica® (Wolfram Research, Inc.), as previously described (Zicha and Dunn, 1995), except that the statistical comparison of the chemotactic responses was based on ANOVA applied to normalised displacement in the direction of the gradient. Furthermore, in RNAi or cDNA expression experiments, the speeds of cell migration were normalised using the average speed of uninjected cells from the same recording.

RNA extraction

Subconfluent, early passaged cells were starved in medium containing reduced (0.5%) serum for 5 hours, followed by (1) no further treatment, (2) stimulation for 30 minutes with 30 ng/ml PDGF and 40 ng/ml IGF or, (3) stimulation for 180 minutes with 30 ng/ml PDGF and 40 ng/ml IGF. Three biological replicates were performed for each condition, and samples were checked for mycoplasma by agar colony growth and found to be free of contamination. Cells were harvested by detachment with trypsin:versene 1:4 and homogenised in Qiashredder columns (Qiagen). To obtain primary tumours, one-million cells per transplant were subcutaneously implanted in rats. After 4-6 weeks the rats were sacrificed, and 1 cm^3 of primary tumour was excised and stored at –20°C in RNAlater (Qiagen). Tumour samples were homogenised for 40 seconds with a rotor-stator homogeniser, then sonicated for 20 seconds, and lysates were cleared of cell debris by centrifugation. Total RNA from cells and tumours was extracted using the RNeasy mini-kit (Qiagen) according to the manufacturer's instructions. Quality of RNA was confirmed by agarose gel electrophoresis.

Microarray analysis

All experiments were performed using Affymetrix Rat 230A GeneChip® oligonucleotide arrays. Briefly, 10 μg of RNA primed with T7-linked oligo(dT) was used to generate first-strand cDNA. After second-strand synthesis, in vitro transcription was performed in the presence of biotinylated UTP and CTP (Enzo Diagnostics), resulting in approximately 65 μg biotinylated cRNA. A complete description of procedures is available upon request. The cRNA was processed as per manufacturer's recommendation using an Affymetrix GeneChip® Instrument System. Briefly, spike controls were added to 10 μg fragmented cDNA before overnight hybridisation. Arrays were then washed and stained with streptavidin-phycoerythrin, before being scanned on an Affymetrix GeneChip® scanner. A complete description of these procedures is available upon request. After scanning, array images were assessed by eye to confirm scanner alignment and the absence of significant bubbles or scratches on the chip surface. 3′-end:5′-end ratios for GAPDH and β-actin were within acceptable limits (from 0.97 to 1.72), and BioB spike controls were found to be present on all chips, with BioC, BioD and CreX also present in increasing intensity. When scaled to a target intensity of 100 (using Affymetrix MAS 5.0 array analysis software), scaling factors for all arrays were within acceptable limits (0.19-0.405), as were background, Q values and mean intensities.

Fluorescence intensity data from The GeneChip® arrays were processed using an algorithm developed in Mathematica® (supplementary material Fig. S1). Genes which the Affymetrix software had classed as 'absent' on each GeneChip® were excluded from the analysis. The fluorescence intensity data were normalised using the median intensity of each chip. The median value of three replicates was calculated, and gene expression was considered in terms of relative changes between cell populations and between different treatments with PDGF-IGF. The *t* test was applied to each relative expression level, and the *P*-value corrected with the Benjamini-Hochberg algorithm (Benjamini and Hochberg, 1995) to avoid excess false-positive calls. There being no significant differences in gene expression in response to PDGF-IGF, the three time-points were averaged and used to calculate the relative expression levels between the four cell populations, with the ANOVA and Benjamini-Hochberg algorithm applied as above. The criteria used to select candidate genes were a relative expression level change of more than 2.5 times ($P<0.05$), with no significant difference in the pattern of gene expression between the cultured cells and the primary tumours. Logged normalised expression values for these genes were calculated and plotted.

RT-PCR

RT-PCR was performed to confirm the gene expression levels indicated by the microarray analysis. Total RNA was extracted from each cell population and reverse-transcribed into cDNA as described above. Fragments of each gene of interest were amplified by PCR using Taq Polymerase (Qiagen). The sequences of the RT-PCR primers are, *Adamts1* forward 5′-GATGGTTTACAGGCTGCCTTC-3′, reverse 5′-TTGTTTGGCACACCAGTAAGC-3′; *Ank3* forward 5′-CCGACTCC-CTCAGACACTACA-3′, reverse 5′-GTGTTCCTTCCAGGTCTCTCC-3′; *Bk* forward 5′-GACCTGATCGCCATAAGGAAG-3′, reverse 5′-GGTTTTGAAGT-GGGGAATCAA-3′; *Cask* forward 5′-ACCATTCGGAAAATCCATGAG-3′, reverse 5′-CTGACACAAGGCCGATAACAA-3′; *Cspg4* forward 5′-ACCATCCA-GAGAGCCACAGTA-3′, reverse 5′-AGCAGGACGTTAGTGAGGACA-3′; *Epb41l3* forward 5′-CATCCAGCAGCAAACTCTCAC-3′, reverse 5′-GTCAC-GAAGGAACAGGGTAGG-3′; *Gapdh* forward 5′-TGCTGAGTATGTCGTG-GAGTCT-3′, reverse 5′-CCCTGTTGCTGTAGCCATATTC-3′; *Grem1* forward 5′-GATGACTGAGAGCGTTGTTCG-3′, reverse 5′-GACCCAGTCACCTTT-CTCTGG-3′; *Plk2* forward 5′-AACTTGGCCAATGCTCTGTTT-3′, reverse 5′-AAGAGCATGTTCAGGGCGTAT-3′; *Ril* forward 5′-AGCAGGCCTGAGAA-CAAGAAC-3′, reverse 5′- TAGCGGAAGGATCCAGACTGT-3′; *Tsnax* forward 5′-AACGCTTGCTATGCCCTTAAA-3′, reverse 5′-CCTTCCACCCAAAATGT-CACT-3′. PCR products were resolved by gel electrophoresis, and visualised by UV transillumination.

Western blotting

Cells were lysed in RIPA buffer containing protease inhibitors for 15 minutes on ice. Lysates were cleared by centrifuging at 10,000 ***g*** for 10 minutes. Protein concentration was measured using the Coomassie assay (Pierce). Equal amounts of protein were resolved by electrophoresis on a 4-12% Novex gel (Invitrogen), transferred to PVDF membrane (Immobilon-P, Millipore) and probed with an antibody to 4.1B (kindly provided by Narla Mohandas, New York Blood Center, NY) using standard immunoblotting and enhanced chemiluminescence protocols. Blots were re-probed with mouse anti-GAPDH or anti-β actin antibody (Abcam) to confirm equal protein loading.

Cloning and expression of 4.1B

Total RNA was extracted from each cell population and reverse-transcribed into cDNA as described above. The full-length cDNA of rat *Epb41l3* was amplified by PCR using a forward primer containing a *Hin*dIII site, 5′-TAAATCAAGCT-TGCAGCAATGACAACCGAATCAGGATCAGACTCAGAA-3′, and a reverse primer containing a *Kpn*I site, 5′-TTAATTGGTACCTGCTGCTCAATCCTC-TCCATCTTCTGGTGTGATTTC-3′, and cloned into pEGFP-C3 (Clontech). To generate an untagged 4.1B construct, the GFP sequence was excised using *Bsr*GI and *Age*I restriction endonucleases, and the ends of the vector made blunt by treatment with mung bean exonuclease, and re-ligated so that untagged 4.1B could be expressed. All nucleases were from New England BioLabs. Cells were transfected with 4.1B or GFP-4.1B construct using Effectene Reagent (Qiagen) according to the manufacturer's instructions and used in experiments after 24 hours. Cells microinjected with the GFP-4.1B construct were used in experiments after 5 hours.

RNA interference

Annealed and purified siRNA oligonucleotides were from Ambion, Inc. and were resuspended according to their protocol. Rat *Epb41l3* gene was targeted by R-

epb41l3 siRNA oligonucleotide with the sequence GCAUGCAGUGCAAAGUGAC. Human *EPB41L3* gene was targeted by H-epb41l3 siRNA1 oligonucleotide with the sequence GCAUCACUAAACCGAUAAU, H-epb41l3 siRNA2 oligonucleotide with the sequence GCUCGAAUAUCAGCAAUUA and H-epb41l3 siRNA3 oligonucleotide with the sequence GCGAUUACAUUAGUGAGUU. The control siRNA was Silencer Negative Control no.1 siRNA (Ambion, Inc.). Chemical transfections of 100 nM siRNA oligonucleotides were carried out using Effectene Reagent (Qiagen) according to the manufacturer's protocol. For microinjection studies, oligonucleotides were labelled with Cy3 using Silencer siRNA Labeling Kit (Ambion, Inc.) and injected at 2 μM. Cells were used in experiments 48 hours after transfection. For RNAi rescue experiments, HeLa cells were transfected with rat 4.1B construct 48 hours after siRNA transfection, and the effects of the rescue assessed after 24 hours (72 hours after the first transfection).

Cytochemistry and laser scanning confocal microscopy

Intact cells, cells transfected with GFP-4.1B construct, and cells microinjected with Cy3-labelled siRNA were fixed in 4% formaldehyde in PBS for 10 minutes, permeabilised in 0.1% Triton X-100 for 10 minutes, stained with Rhodamine-phalloidin or Alexa Fluor-488–phalloidin at 1:2000 dilution for 30 minutes, and then mounted in Mowiol. Randomly selected images were acquired on a Zeiss LSM 510 laser scanning confocal microscope with a 63× NA 1.4 phase-contrast objective lens. Quantitative analysis of the incidence of actin stress fibres was conducted using a blind protocol. T15 cells microinjected with a mixture of GFP and 4.1B expression constructs were fixed after 5 hours in 4% formaldehyde in PBS for 10 minutes and fluorescence images were acquired as above. Simultaneously with GFP fluorescence we visualised interference reflection images using the 488 nm line of an argon laser with no emission filter in front of a second detector.

We are grateful to Peter Parker, Anne Ridley and Michael Way for helpful discussions and support throughout the project, to Trevor Duhig and Alastair Nicol for comments on the manuscript, and to Deborah Aubyn and Peter Jordan for help with microscopy.

References

Ahmad, A. and Hart, I. R. (1997). Mechanisms of metastasis. *Crit. Rev. Oncol. Hematol.* **26**, 163-173.

Benjamini, Y. and Hochberg, Y. (1995). Controlling the false discovery rate: a practical and powerful approach to multiple testing. *J. R. Stat. Soc. Ser. B* **57**, 289-300.

Bourguignon, L. Y., Zhu, H., Shao, L. and Chen, Y. W. (2000). Ankyrin-Tiam1 interaction promotes Rac1 signaling and metastatic breast tumor cell invasion and migration. *J. Cell Biol.* **150**, 177-191.

Burg, M. A., Grako, K. A. and Stallcup, W. B. (1998). Expression of the NG2 proteoglycan enhances the growth and metastatic properties of melanoma cells. *J. Cell. Physiol.* **177**, 299-312.

Charboneau, A. L., Singh, V., Yu, T. and Newsham, I. F. (2002). Suppression of growth and increased cellular attachment after expression of DAL-1 in MCF-7 breast cancer cells. *Int. J. Cancer* **100**, 181-188.

Chen, B., Blair, D. G., Plisov, S., Vasiliev, G., Perantoni, A. O., Chen, Q., Athanasiou, M., Wu, J. Y., Oppenheim, J. J. and Yang, D. (2004). Cutting edge: bone morphogenetic protein antagonists Drm/Gremlin and Dan interact with Slits and act as negative regulators of monocyte chemotaxis. *J. Immunol.* **173**, 5914-5917.

Chenna, R., Sugawara, H., Koike, T., Lopez, R., Gibson, T. J., Higgins, D. G. and Thompson, J. D. (2003). Multiple sequence alignment with the Clustal series of programs. *Nucleic Acids Res.* **31**, 3497-3500.

Clark, E. A., Golub, T. R., Lander, E. S. and Hynes, R. O. (2000). Genomic analysis of metastasis reveals an essential role for RhoC. *Nature* **406**, 532-535.

Conboy, J. G. (1993). Structure, function, and molecular genetics of erythroid membrane skeletal protein 4.1 in normal and abnormal red blood cells. *Semin. Hematol* **30**, 58-73.

Ein-Dor, L., Zuk, O. and Domany, E. (2006). Thousands of samples are needed to generate a robust gene list for predicting outcome in cancer. *Proc. Natl. Acad. Sci. USA* **103**, 5923-5928.

Fidler, I. J. and Hart, I. R. (1982). Biological diversity in metastatic neoplasms: origins and implications. *Science* **217**, 998-1003.

Gascard, P., Parra, M. K., Zhao, Z., Calinisan, V. R., Nunomura, W., Rivkees, S. A., Mohandas, N. and Conboy, J. G. (2004). Putative tumor suppressor protein 4.1B is differentially expressed in kidney and brain via alternative promoters and 5′ alternative splicing. *Biochim. Biophys. Acta* **1680**, 71-82.

Gildea, J. J., Seraj, M. J., Oxford, G., Harding, M. A., Hampton, G. M., Moskaluk, C. A., Frierson, H. F., Conaway, M. R. and Theodorescu, D. (2002). RhoGDI2 is an invasion and metastasis suppressor gene in human cancer. *Cancer Res.* **62**, 6418-6423.

Gutmann, D. H., Donahoe, J., Perry, A., Lemke, N., Gorse, K., Kittiniyom, K., Rempel, S. A., Gutierrez, J. A. and Newsham, I. F. (2000). Loss of DAL-1, a protein 4.1-related tumor suppressor, is an important early event in the pathogenesis of meningiomas. *Hum. Mol. Genet.* **9**, 1495-1500.

Gutmann, D. H., Hirbe, A. C., Huang, Z. Y. and Haipek, C. A. (2001). The protein 4.1 tumor suppressor, DAL-1, impairs cell motility, but regulates proliferation in a cell-type-specific fashion. *Neurobiol. Dis.* **8**, 266-278.

Khanna, C., Khan, J., Nguyen, P., Prehn, J., Caylor, J., Yeung, C., Trepel, J., Meltzer, P. and Helman, L. (2001). Metastasis-associated differences in gene expression in a murine model of osteosarcoma. *Cancer Res.* **61**, 3750-3759.

Khanna, C., Wan, X., Bose, S., Cassaday, R., Olomu, O., Mendoza, A., Yeung, C., Gorlick, R., Hewitt, S. M. and Helman, L. J. (2004). The membrane-cytoskeleton linker ezrin is necessary for osteosarcoma metastasis. *Nat. Med.* **10**, 182-186.

Kikuchi, S., Yamada, D., Fukami, T., Masuda, M., Sakurai-Yageta, M., Williams, Y. N., Maruyama, T., Asamura, H., Matsuno, Y., Onizuka, M. et al. (2005). Promoter methylation of DAL-1/4.1B predicts poor prognosis in non-small cell lung cancer. *Clin. Cancer Res.* **11**, 2954-2961.

Kikuchi, S., Yamada, D., Fukami, T., Maruyama, T., Ito, A., Asamura, H., Matsuno, Y., Onizuka, M. and Murakami, Y. (2006). Hypermethylation of the TSLC1/IGSF4 promoter is associated with tobacco smoking and a poor prognosis in primary nonsmall cell lung carcinoma. *Cancer* **106**, 1751-1758.

Kittiniyom, K., Gorse, K. M., Dalbegue, F., Lichy, J. H., Taubenberger, J. K. and Newsham, I. F. (2001). Allelic loss on chromosome band 18p11.3 occurs early and reveals heterogeneity in breast cancer progression. *Breast Cancer Res.* **3**, 192-198.

Kuno, K., Bannai, K., Hakozaki, M., Matsushima, K. and Hirose, K. (2004). The carboxyl-terminal half region of ADAMTS-1 suppresses both tumorigenicity and experimental tumor metastatic potential. *Biochem. Biophys. Res. Commun.* **319**, 1327-1333.

Lee, J. E., Kim, H. J., Bae, J. Y., Kim, S. W., Park, J. S., Shin, H. J., Han, W., Kang, K. S. and Noh, D. Y. (2005). Neogenin expression may be inversely correlated to the tumorigenicity of human breast cancer. *BMC Cancer* **5**, 154.

Parra, M., Gascard, P., Walensky, L. D., Snyder, S. H., Mohandas, N. and Conboy, J. G. (1998). Cloning and characterization of 4.1G (EPB41L2), a new member of the skeletal protein 4.1 (EPB41) gene family. *Genomics* **49**, 298-306.

Peracaula, R., Cleary, K. R., Lorenzo, J., de Llorens, R. and Frazier, M. L. (2000). Human pancreatic ribonuclease **1**, expression and distribution in pancreatic adenocarcinoma. *Cancer* **89**, 1252-1258.

Pokorna, E., Jordan, P. W., O'Neill, C. H., Zicha, D., Gilbert, C. S. and Vesely, P. (1994). Actin cytoskeleton and motility in rat sarcoma cell populations with different metastatic potential. *Cell Motil. Cytoskeleton* **28**, 25-33.

Ramaswamy, S., Ross, K. N., Lander, E. S. and Golub, T. R. (2003). A molecular signature of metastasis in primary solid tumors. *Nat. Genet.* **33**, 49-54.

Sahai, E., Wyckoff, J., Philippar, U., Segall, J. E., Gertler, F. and Condeelis, J. (2005). Simultaneous imaging of GFP, CFP and collagen in tumors in vivo using multiphoton microscopy. *BMC Biotechnol.* **5**, 14.

Syed, N., Smith, P., Sullivan, A., Spender, L. C., Dyer, M., Karran, L., O'Nions, J., Allday, M., Hoffmann, I., Crawford, D. et al. (2006). Transcriptional silencing of Polo-like kinase 2 (SNK/PLK2) is a frequent event in B-cell malignancies. *Blood* **107**, 250-256.

Topol, L. Z., Marx, M., Laugier, D., Bogdanova, N. N., Boubnov, N. V., Clausen, P. A., Calothy, G. and Blair, D. G. (1997). Identification of drm, a novel gene whose expression is suppressed in transformed cells and which can inhibit growth of normal but not transformed cells in culture. *Mol. Cell. Biol.* **17**, 4801-4810.

Tran, Y. K., Bogler, O., Gorse, K. M., Wieland, I., Green, M. R. and Newsham, I. F. (1999). A novel member of the NF2/ERM/4.1 superfamily with growth suppressing properties in lung cancer. *Cancer Res.* **59**, 35-43.

Vallenius, T., Scharm, B., Vesikansa, A., Luukko, K., Schafer, R. and Makela, T. P. (2004). The PDZ-LIM protein RIL modulates actin stress fiber turnover and enhances the association of alpha-actinin with F-actin. *Exp. Cell Res.* **293**, 117-128.

van de Vijver, M. J., He, Y. D., van't Veer, L. J., Dai, H., Hart, A. A., Voskuil, D. W., Schreiber, G. J., Peterse, J. L., Roberts, C., Marton, M. J. et al. (2002). A gene-expression signature as a predictor of survival in breast cancer. *N. Engl. J. Med.* **347**, 1999-2009.

van't Veer, L. J., Dai, H., van de Vijver, M. J., He, Y. D., Hart, A. A., Mao, M., Peterse, H. L., van der Kooy, K., Marton, M. J., Witteveen, A. T. et al. (2002). Gene expression profiling predicts clinical outcome of breast cancer. *Nature* **415**, 530-536.

Vesely, P. and Weiss, R. A. (1973). Cell locomotion and contact inhibition of normal and neoplastic rat cells. *Int. J. Cancer* **11**, 64-76.

Vesely, P., Chaloupkova, A., Urbanec, P., Urbancova, H., Bohac, L., Krchnakova, E., Franc, F., Sprincl, L., Vousden, K., Moss, R. et al. (1987). Patterns of in vitro behaviour characterizing cells of spontaneously metastasizing K2M rat sarcoma. *Folia Biol. Praha* **33**, 307-324.

Wyckoff, J. B., Jones, J. G., Condeelis, J. S. and Segall, J. E. (2000). A critical step in metastasis: in vivo analysis of intravasation at the primary tumor. *Cancer Res.* **60**, 2504-2511.

Zicha, D. and Dunn, G. A. (1995). Are growth factors chemotactic agents? *Exp. Cell Res.* **221**, 526-529.

Zicha, D., Dunn, G. A. and Brown, A. F. (1991). A new direct-viewing chemotaxis chamber. *J. Cell Sci.* **99**, 769-775.